ADVANCES IN NUCLEAR SCIENCE AND APPLICATIONS

Volume 2, No. 2 (2026), P. 121-138

Time-of-flight $\Delta E - E$ spectrometer for registration of nuclear reaction products

D. Aznabayev[1,2,*], S.M. Lukyanov[1], T. Issatayev[1,2], V.A. Maslov[1], E.V. Melnik[1], K. Mendibayev[1,2], A.V. Shakhov[1], A.M. Zolotorev[1], and D. Alimov[2]

[1]Joint Institute for Nuclear Research, Dubna, Russia

[2]Institute of Nuclear Physics, Almaty, Kazakhstan

e-mail: daur_is101@jinr.ru

DOI: 10.63907/ansa.v2i2.83
Received: 18 May 2026

Abstract

This work presents the results of testing a newly developed time-of-flight $\Delta E - E$ spectrometer designed to measure the time-of-flight (TOF) and ionization energy losses (ΔE) of charged particles. The detector system makes it possible to determine the particle mass and obtain information on the charge of the registered particles. The performance of the detector system was verified using a ^{226}Ra source and spontaneous fission fragments from a ^{252}Cf source. The obtained results demonstrate the capability of the system to measure the parameters of both light charged particles and fission fragments produced in heavy-ion nuclear reactions. The influence of key system parameters, including detector time resolution, accuracy of energy-loss measurements, and the gas filling of the ionization chamber, on the overall resolution of the spectrometer is evaluated. The registered particle spectra are analyzed, and methodological aspects of data processing are discussed. The work is aimed at further optimization of the spectrometer and expansion of its capabilities for detailed analysis of heavy-nucleus fission products in upcoming experiments at the MAVR setup.

1 Introduction

Accurate identification of nuclear reaction products by their mass A and charge Z is essential for studying nuclear structure, shell effects, and reaction mechanisms. Significant progress in experimental techniques has made it possible to perform high-precision mass measurements of exotic nuclides with relative accuracies reaching 10^{-6}. For this purpose, time-of-flight systems with long flight paths, as well as gas-filled ionization chambers with large apertures capable of measuring specific energy loss and residual energy, are widely used.

However, in studies of mass and charge distributions of nuclear reaction products, primarily fission fragments of heavy nuclei, such extremely high precision is not always required. In this case, compact time-of-flight spectrometers based on fast timing detectors, such as microchannel plates (MCPs), gas avalanche counters, and similar devices, are effective tools. Their capabilities have been demonstrated in experiments performed with the CORSET spectrometer [1] and the Dubna double-arm time-of-flight spectrometer [2], where mass distributions of fission fragments were obtained and processes such as quasifission, fast fission, deep-inelastic nucleon transfer, and the influence of shell structure on fragment formation were investigated.

Fission fragments carry important information on fission-barrier parameters, deformation of the initial nucleus, separation dynamics, and Coulomb repulsion effects. Their kinetic energies, mass and charge distributions, as well as correlations between these quantities, provide important constraints for fission models and make it possible to study the influence of excitation energy on the disappearance of shell effects. This is especially relevant for heavy-ion reactions with heavy targets, where the compound-nucleus fission channel can play a dominant role.

Registration of fission fragments using the TOF method presents significant experimental challenges. High-precision mass reconstruction requires optimized working conditions, including ultrathin entrance windows, proper gas pressure, increased MCP anode voltage, and improved timing resolution. Addressing these requirements calls for a dedicated $\Delta E - E$ spectrometer capable of simultaneous measurement of TOF, energy loss, and residual energy.

The present work is devoted to the development, testing, and calibration of a TOF $\Delta E - E$ spectrometer designed to measure the time-of-flight (TOF), energy loss (ΔE), and residual energy (E) of charged particles, enabling determination of their mass and charge. The obtained calibration data represent an essential step toward experiments with extracted accelerator beams.

The efficiency of the TOF method for studying reaction products was demonstrated in the work of Auger *et al.* [3], where high-resolution mass–charge distributions were obtained in the reaction $^{40}\mathrm{Ar} + {}^{238}\mathrm{U}$ at a beam energy of 926 MeV. The reported spectra showed clear isotopic separation of fragments in the mass range $A = 31$–40 with a mass resolution of $\Delta M \lesssim 1$ a.m.u. This example highlights the potential of TOF spectroscopy for direct observation of fine structures in mass distributions and for investigation of multinucleon transfer mechanisms.

In the near future, the developed setup is planned to be used in experiments with the reactions $^{40,48}\mathrm{Ca} + {}^{197}\mathrm{Au}$. These measurements will make it possible to extract mass–charge distributions for elements with $Z = 20$–28, including separation of isotopic channels of multinucleon transfer.

Thus, the detector system developed in this work is intended not only for studying

fission fragments of heavy nuclei but also for investigating multinucleon transfer reactions and heavy-ion reaction products in general. The achieved technical characteristics demonstrate the efficiency of the spectrometer and confirm its applicability for future experiments devoted to fission mechanisms, nucleon transfer, and formation of exotic nuclei.

2 Experimental Setup

The parameters of fission fragments produced in heavy-ion nuclear reactions were measured using the developed TOF $\Delta E - E$ spectrometer. The spectrometer consists of a start detector based on microchannel plates in an electrostatic mirror configuration (MCP) [4], an ionization chamber (IC), and a silicon semiconductor detector (Si), as shown in Figure 1. The operating principle is based on measuring the time of flight (TOF) between the MCP start detector and the Si stop detector, as well as determining the energy loss (ΔE) in the ionization chamber and the residual energy (E) in the silicon detector.

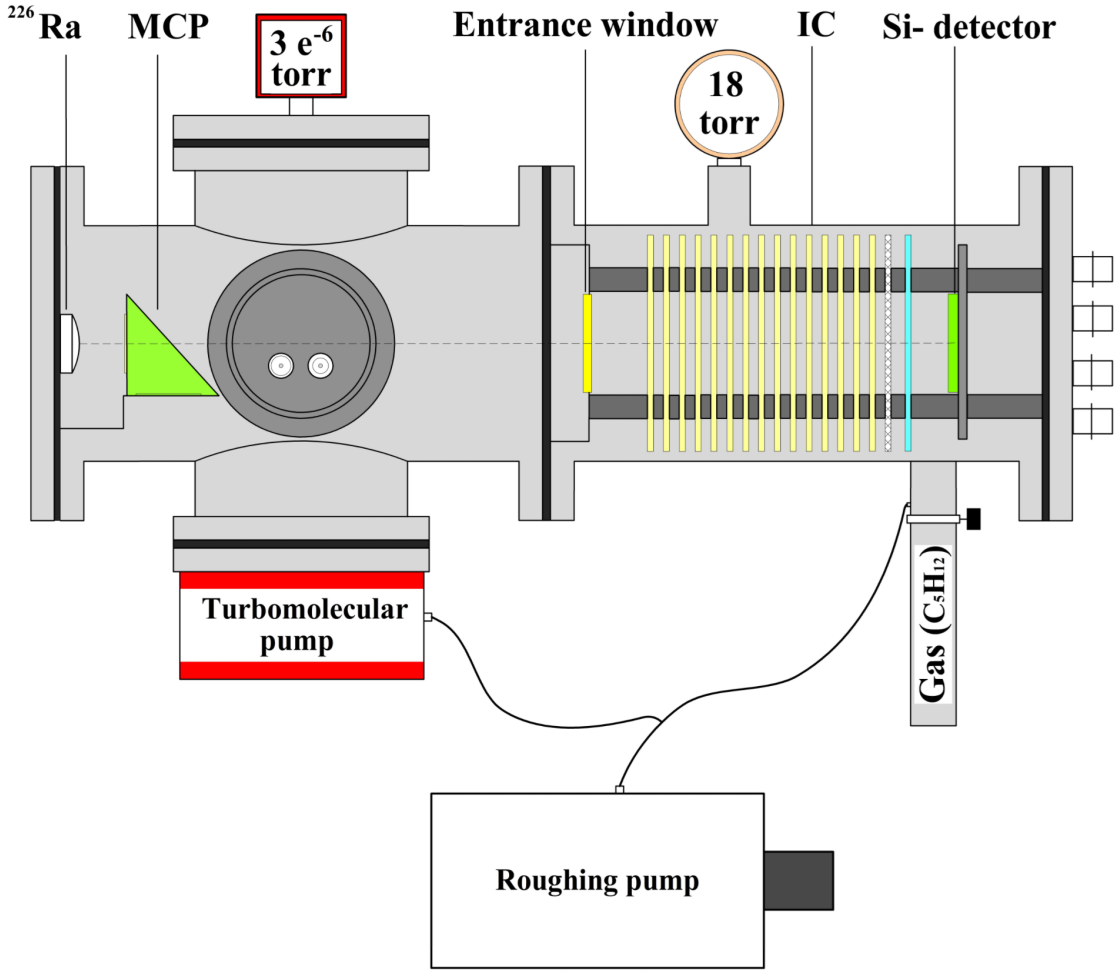

Figure 1: Schematic diagram of the experimental setup.

A high vacuum of about 10^{-6} Torr inside the reaction chamber of the spectrometer, required for stable MCP operation, was maintained using a fore-vacuum pump and a turbomolecular pump. The vacuum in the gas section of the ionization

chamber, down to about 10^{-3} Torr, was provided by a fore-vacuum pump. Gas filling and pressure regulation of the ionization chamber were performed using a specially designed gas handling system [5].

2.1 MCP-Based Detector

The start detector is a key element of the time-of-flight technique and must provide high time resolution, low sensitivity to the background of light particles, minimal energy losses during the registration of heavy reaction products, and resistance to radiation damage. These requirements are satisfied by a detector based on microchannel plates (MCPs). The MCPs used in the detector had a thickness of 0.8 mm and a diameter of 33 mm.

The detector consisted of an entrance emission foil made of Mylar with a thickness of 120 μg/cm^2, coated with a 30 μg/cm^2 gold layer, an accelerating grid of the electrostatic mirror, and a chevron assembly formed by two microchannel plates.

In the MCP detector, a particle passing through the emission foil ejects secondary electrons, which are then accelerated in the electric field between the foil and the accelerating grid. The grid provides nearly isochronous transport of the electrons, thereby minimizing their time spread.

In the region of the electrostatic mirror, the accelerated electrons are deflected by 90°, after which they are registered by the MCP assembly, as shown in Figure 2.

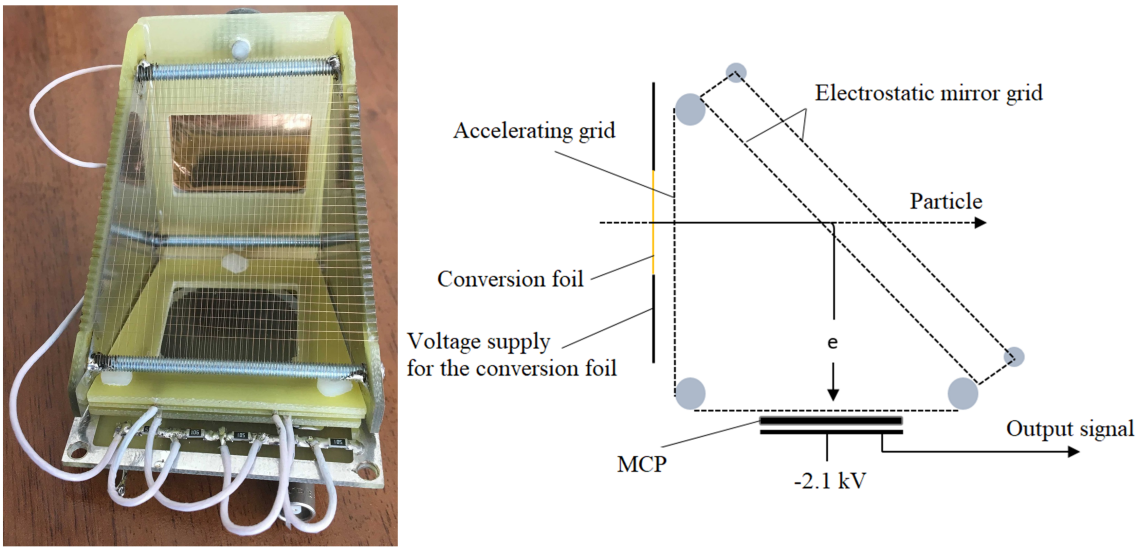

Figure 2: MCP start detector and its operating principle.

2.2 Ionization chamber design

In our methodology, the ionization chamber (IC) serves as one of the main detectors for the registration of charged particles and the measurement of their energy characteristics. An ionization chamber with a longitudinal electric field directed along the trajectory of the registered particle was used [6].

The design of the ionization chamber includes the following elements:

- an entrance window with a thickness of 3 μm, which separates the gas-filled region from the vacuum and allows particles to enter the IC volume;

- a cathode with a thickness of 3 μm, made of thin aluminized Mylar foil, through which the charged particle passes and initiates gas ionization;
- an electrode system consisting of double-sided fiberglass (glass-epoxy) plates with a thickness of 3 mm, which provides the formation of a uniform electric field;
- a Frisch grid used for shielding the anode;
- an anode with a thickness of 3 μm, made of aluminized Mylar foil, which collects the signal from electrons passing through the Frisch grid;
- a silicon semiconductor detector with dimensions of 50×50 mm^2 and a thickness of 625 μm, mounted separately on the rear flange.

A block diagram of the developed ionization chamber detector is shown in Figure 3.

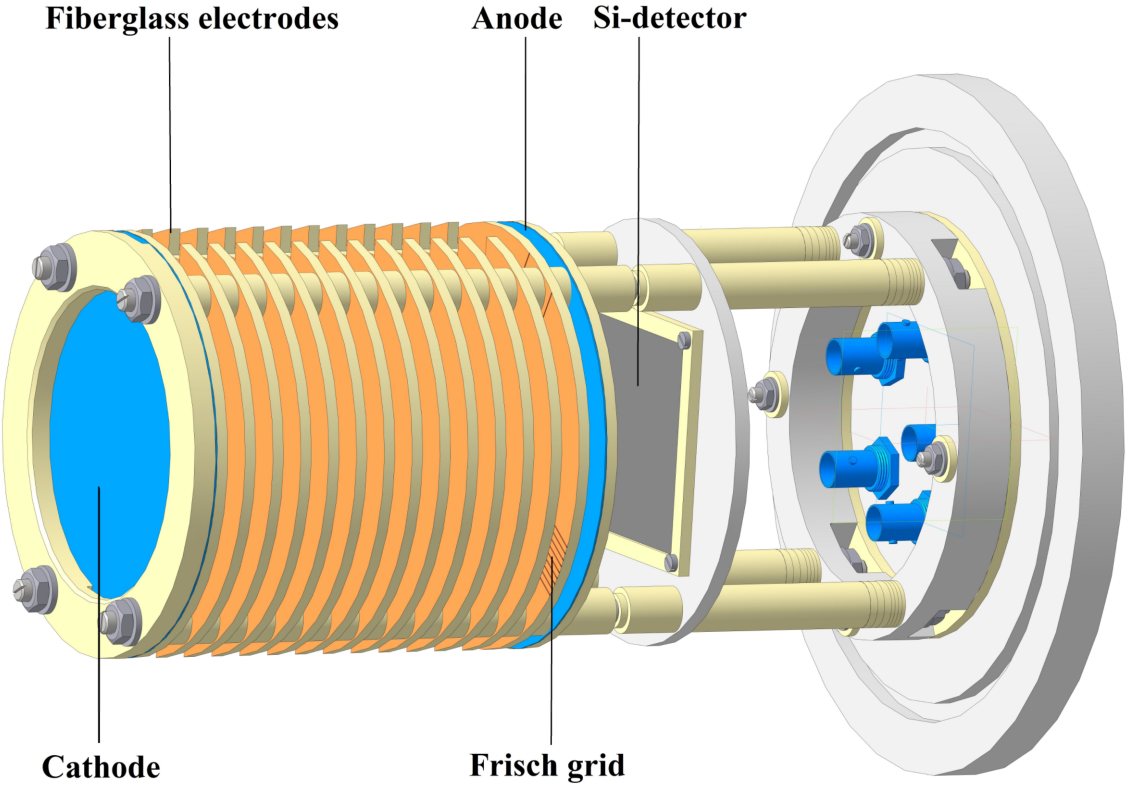

Figure 3: Design of the ionization chamber detector.

Twelve field-shaping fiberglass rings were used in the ionization chamber (IC) and connected through 100 MΩ resistors. In this configuration, the voltage drop between adjacent rings remained constant. The rings were separated by 5-mm-thick Teflon spacers and fixed by insulating rods, providing electrical insulation. This design ensured a uniform electric field distribution and nearly parallel electric field lines inside the active volume of the chamber.

A distance of approximately 7 mm between the Frisch grid and the anode was maintained using Teflon spacers. The resistor connecting the anode to the Frisch grid had a resistance of 200 MΩ, which was twice the resistance of the field-shaping ring resistors.

The Frisch grid screened the anode from the motion of ions and electrons until the electrons crossed the grid. As a result, the anode signal was formed only when the electrons passed through the Frisch grid, making the signal practically independent of the primary ionization position inside the chamber.

Signals from the cathode were transmitted directly through a cable and a vacuum-tight SR-50 connector to the preamplifier. Signals from the Frisch grid were also extracted through vacuum-tight SR-50 connectors.

The operating principle of such chambers is based on the ionization of gas atoms by passing charged particles, resulting in the formation of ion–electron pairs. The motion of these charges in the electric field of the detector produces a measurable current signal.

One of the key parameters for analyzing particle–matter interactions and for particle identification is the specific energy loss, $\mathrm{d}E/\mathrm{d}x$, which characterizes the energy lost by a particle per unit path length in the medium. The particle charge also plays a crucial role, since it determines the interaction strength with matter and enables charge identification. In the nonrelativistic approximation, the specific energy loss can be written in the following proportional form:

$$\frac{\mathrm{d}E}{\mathrm{d}x} \sim \frac{Z^2}{v^2} \sim \frac{MZ^2}{E}, \tag{1}$$

where $\mathrm{d}E/\mathrm{d}x$ is the specific energy loss per unit path length, Z is the particle charge, v is the particle velocity, M is the particle mass, and E is the kinetic energy of the particle.

A necessary condition for the operation of the ionization chamber is gas filling. In the present experiment, pentane, $\mathrm{C_5H_{12}}$, was used as the working gas at adjustable pressures in the range from 5 to 300 Torr. The operating pressure of the ionization chamber was varied from 10 to 300 Torr depending on the energy E and atomic number Z of the detected particles. The optimal pressure range was found to be 10–30 Torr, since it minimizes multiple scattering of charged particles in the gas and ensures stable measurement of the energy loss ΔE.

2.3 Entrance Window Design

The detected particle enters the gas volume through an entrance window consisting of a thin Mylar foil with a thickness of 3–10 μm. The window thickness was chosen to minimize energy losses and energy straggling while ensuring sufficient mechanical stability.

The Mylar window was reinforced with a special mesh support structure to prevent stretching and rupture due to the pressure difference between the ionization chamber and the high-vacuum region of the beamline. For this purpose, a dedicated support frame inserted into the window holder was developed. This design makes it possible to minimize the initial energy losses of incoming particles and significantly reduce their energy spread. Details of this construction are shown in Figure 4.

2.4 Application of a Silicon Semiconductor Detector in the TOF $\Delta E - E_r$ Spectrometer

The silicon semiconductor detector (Si) is an integral component of the spectrometer, providing precise measurements of the residual energy E_r of charged particles, as

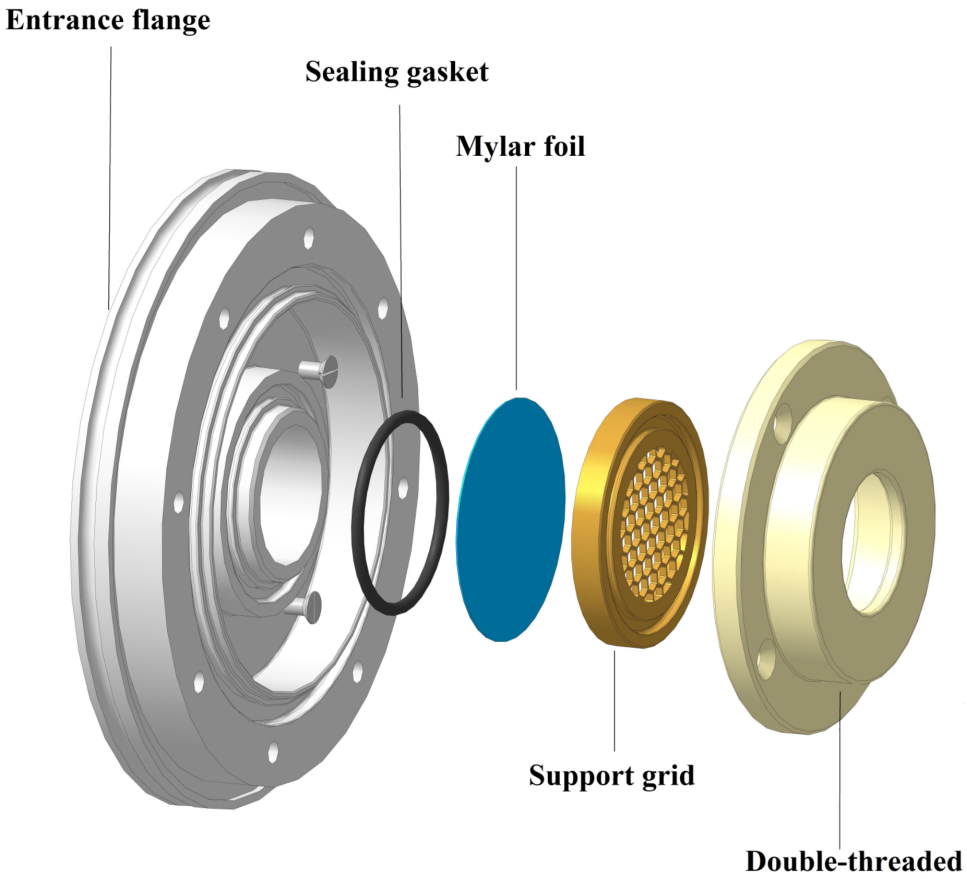

Figure 4: Design of the entrance window.

well as timing characteristics of the detected events.

The main functions and characteristics of the silicon semiconductor detector used in this work are as follows:

- active area of 50×50 mm^2;
- thickness of 625 μm, allowing efficient detection of charged particles over a wide energy range;
- high energy resolution, which is important for the spectrometry of light charged particles and fission fragments of heavy nuclei;
- measurement of the residual energy of particles passing through the ionization chamber (IC), enabling their identification;
- time-of-flight registration with high precision, required for correlation with signals from the microchannel plate (MCP) detector.

Due to its high energy resolution, the silicon detector makes it possible to discriminate between particles of different types and energies, making it a key element of the TOF $\Delta E - E_r$ spectrometer.

Figure 5: Silicon semiconductor detector used as a stop detector in the TOF $\Delta E - E_r$ spectrometer.

3 Calibration and Experimental Studies

The detector system was calibrated using alpha particles with well-defined initial energies emitted by a ^{226}Ra radioactive source. This procedure made it possible to tune the timing and energy responses of the detectors and to evaluate the influence of the ionization chamber gas on the overall spectrometer resolution. The alpha-particle energy spectrum of ^{226}Ra, measured with the silicon semiconductor detector (Si), was used for energy calibration and for determining the accuracy of residual-energy measurements. The residual energies were calculated using the LISE++ software package [7], taking into account all energy losses of the alpha particles in the detector system. The obtained spectrum is shown in Figure 6. The energy resolution of the silicon detector was approximately 100 keV.

The velocity of alpha particles was determined using two detectors: a start MCP detector and a stop Si detector. The flight path length between the detectors was 55 cm. The time of flight of alpha particles was calculated using the following expression:

$$t\ [\text{ns}] = 72.3\, d\ [\text{m}] \sqrt{\frac{A\ [\text{a.m.u.}]}{E\ [\text{MeV}]}}, \tag{2}$$

where t is the time of flight, d is the flight path length, A is the particle mass, and E is the kinetic energy.

The time distribution of alpha particles recorded by the experimental setup is shown in Figure 7. In this case, the time resolution (FWHM) was 400 ps, which enabled clear separation of all energy peaks of ^{226}Ra. The test results are presented in Figure 8 as a two-dimensional spectrum showing the correlation between the energy and time of flight of alpha particles. The observed correlation confirms the correct operation of the start MCP detector and the Si stop detector in the time-of-flight

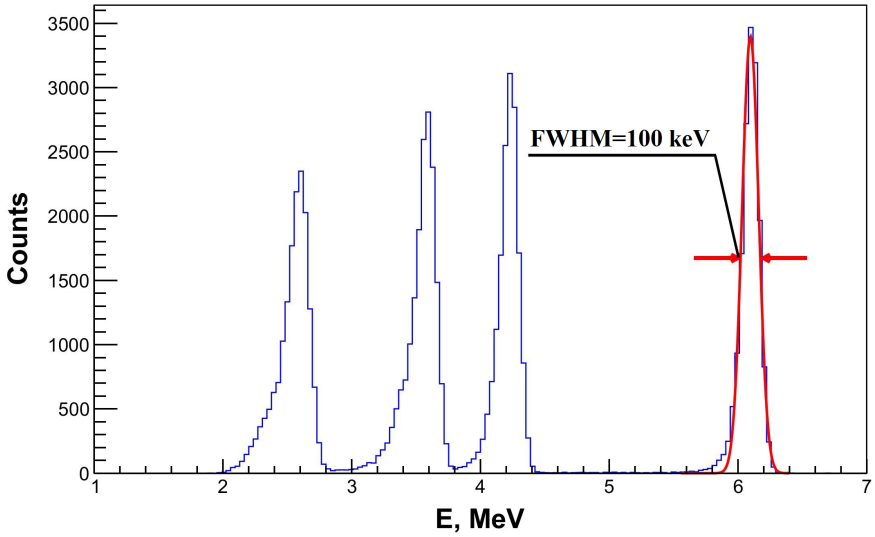

Figure 6: Energy distribution of alpha particles from the ^{226}Ra source registered by the silicon semiconductor detector.

measurement mode.

Integration of the ionization chamber into the spectrometer, which allows measurement of the corresponding energy losses ΔE in the chamber, significantly improves particle separation in energy. In this case, the combination of the residual energy measured by the Si detector and the energy loss in the gas volume provides additional information on the specific ionization of the registered particles. This is especially important for separating particles with close residual energies but different energy losses in the ionization chamber. Based on these data, a two-dimensional distribution of alpha particles detected by the Si detector was constructed. This distribution illustrates the dependence of the residual energy E_r on the corresponding energy loss ΔE in the ionization chamber, as shown in Figure 9. The observed structure of the two-dimensional spectrum demonstrates the applicability of the $\Delta E - E_r$ method for particle identification and confirms the correct operation of the ionization chamber as part of the developed TOF $\Delta E - E_r$ spectrometer.

The experimental setup configuration employing the ionization chamber significantly improves the spectrometer resolution and enables not only time-of-flight measurements of particles but also their charge identification, as shown in Figure 9.

Charge identification of the detected alpha particles was performed by further data analysis based on the Bethe–Bloch relation:

$$\frac{\mathrm{d}E}{\mathrm{d}x} \sim \frac{z^2}{v^2}, \tag{3}$$

where z is the particle charge, v is its velocity, and $\mathrm{d}E/\mathrm{d}x$ is the specific energy loss.

The particle velocity was determined using the relation

$$v = \frac{d}{t}, \tag{4}$$

where $d = 55$ cm is the flight path between the start and stop detectors, and t is the time of flight.

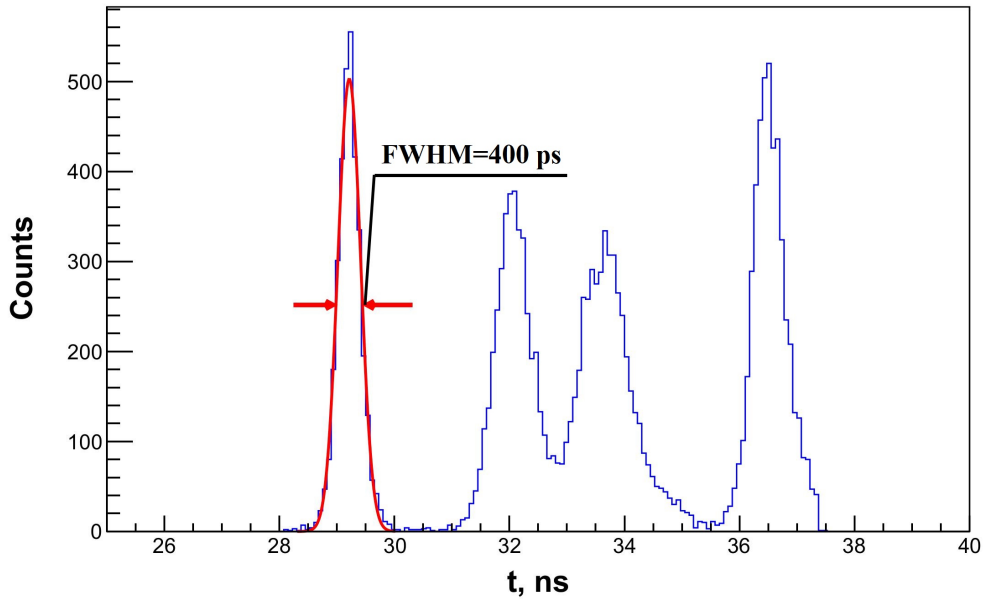

Figure 7: Time distribution of alpha particles from the ^{226}Ra source.

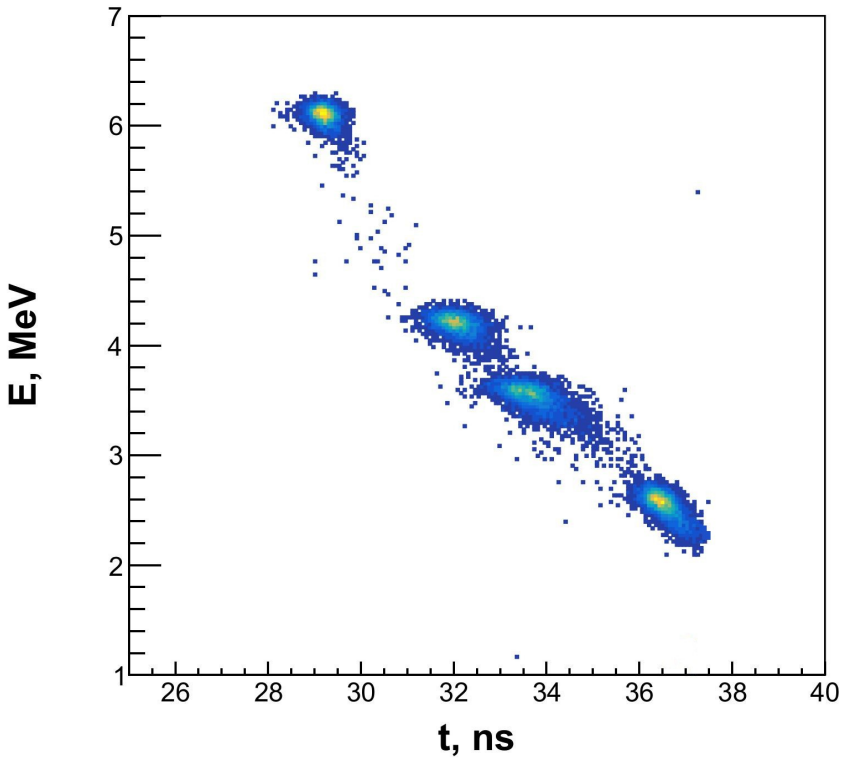

Figure 8: Correlation between the energy and time of flight of alpha particles recorded using the start MCP detector and the Si stop detector.

Based on Eqs. (3) and (4), the charge of the identified particle can be expressed in proportional form as

$$z \sim \frac{d}{t}\sqrt{\frac{\mathrm{d}E}{\mathrm{d}x}}. \tag{5}$$

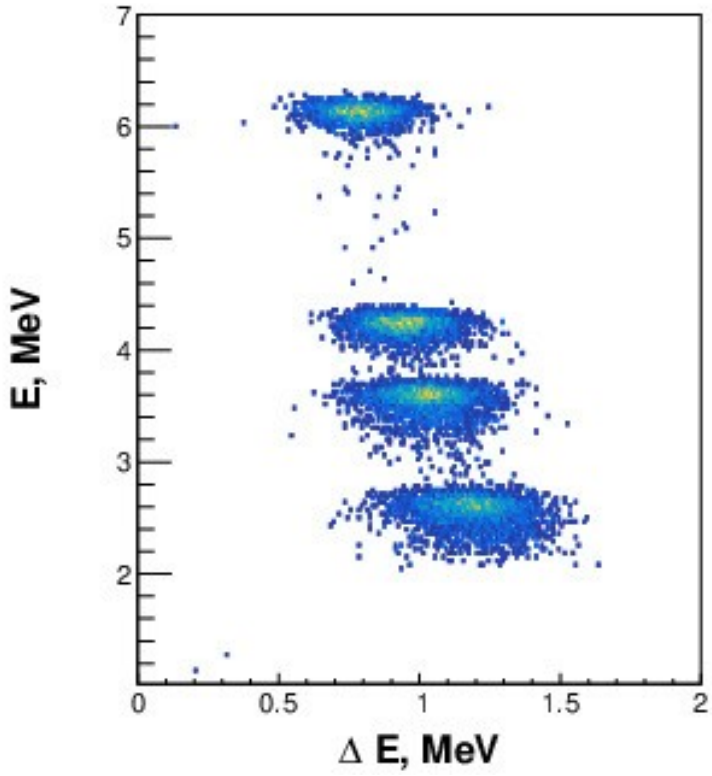

Figure 9: Two-dimensional distribution of alpha particles showing the correlation between the residual energy E_r measured by the Si detector and the energy loss ΔE in the ionization chamber.

The calculated values of the time of flight (TOF), specific energy loss, and charge for alpha particles from the ^{226}Ra source are presented in Table 1. The obtained charge values are clustered around $Z \approx 2$, which corresponds to alpha particles. This confirms the reliability of the measurements and the stable operation of the detection system.

Calibration of the detection system made it possible to determine the charge distribution of the detected particles as a function of their time of flight, as shown in Figure 10. The resulting distribution clearly demonstrates that the identified particles are concentrated around $Z \approx 2$, in agreement with the expected charge of alpha particles.

Table 1: Calculated values of the time of flight (TOF), specific energy loss, and charge for alpha particles from the ^{226}Ra source.

^{226}Ra	TOF, ns	$\mathrm{d}E/\mathrm{d}x$, MeV/cm	Z
α_1	28.848	0.05976	1.86
α_2	32.200	0.07288	1.84
α_3	34.224	0.08172	1.84
α_4	36.038	0.09070	1.84

The uncertainties of the charge and mass determination were estimated by propagating the main experimental contributions from the time-of-flight, flight-path

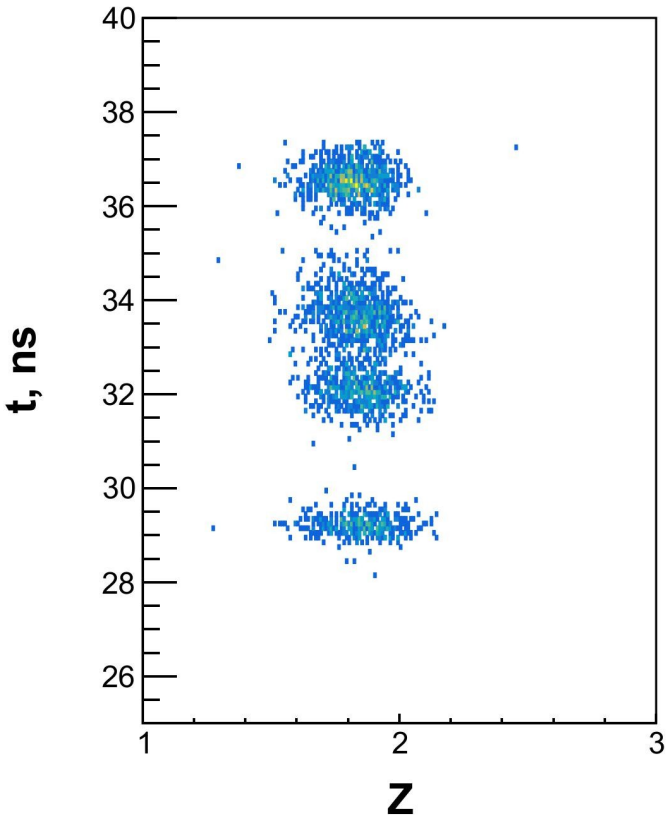

Figure 10: Dependence of the particle charge on the time of flight.

length, and energy-loss measurements. For charge identification, Eq. (5) gives

$$z \sim \frac{d}{t}\sqrt{\frac{\mathrm{d}E}{\mathrm{d}x}}, \tag{6}$$

where d is the flight path and t is the measured time of flight. Assuming independent uncertainties, the relative uncertainty can be written as

$$\left(\frac{\Delta z}{z}\right)^2 = \left(\frac{\Delta d}{d}\right)^2 + \left(\frac{\Delta t}{t}\right)^2 + \frac{1}{4}\left(\frac{\Delta(\mathrm{d}E/\mathrm{d}x)}{\mathrm{d}E/\mathrm{d}x}\right)^2. \tag{7}$$

For the present geometry, $d = 55$ cm, and the measured time resolution was about 400 ps FWHM, corresponding to $\sigma_t \approx 0.17$ ns. For alpha-particle times of flight in the range of 28.8–36.0 ns, the timing contribution to $\Delta z/z$ is below 1%. Therefore, the dominant contribution comes from the uncertainty of the energy-loss measurement in the ionization chamber, including gas-pressure stability, calibration of the ionization signal, entrance-window thickness, and energy straggling. Experimental stopping-power and energy-loss measurements for MeV-range heavy-ion beams generally have absolute uncertainties of several percent. For example, ICRU Report 73 summarizes stopping-power data for ions heavier than helium [8], while dedicated energy-loss measurements show that the final accuracy depends on the experimental method, target thickness, detector calibration, and corrections for energy losses in foils and detector materials [9]. In the present work, corrections for energy losses and ranges in detector materials were also estimated using SRIM calculations [10]. Taking these factors into account, the uncertainty of the energy-loss measurement in the present

test configuration was estimated to be about 12–15%. This results in a charge uncertainty of approximately $\Delta z/z \approx 6$–8%. For alpha particles, this corresponds to $\Delta Z \approx 0.12$–0.16, while for fission fragments with $Z \approx 50$, it corresponds to about 3–4 charge units.

The fragment masses were reconstructed using the TOF–E relation

$$M = \frac{2E_{\text{tot}}}{v^2} = 2E_{\text{tot}} \left(\frac{t}{d}\right)^2, \tag{8}$$

where E_{tot} is the sum of the residual energy measured by the silicon detector and the energy loss in the ionization chamber, including corrections for energy losses in detector materials. The corresponding relative uncertainty can be estimated as

$$\left(\frac{\Delta M}{M}\right)^2 = \left(\frac{\Delta E_{\text{tot}}}{E_{\text{tot}}}\right)^2 + 4\left(\frac{\Delta t}{t}\right)^2 + 4\left(\frac{\Delta d}{d}\right)^2. \tag{9}$$

The statistical contribution from the timing resolution is about 1–2% for the measured time-of-flight range. The dominant systematic uncertainty is associated with the total energy reconstruction, including calibration of the silicon detector, the energy-loss signal in the ionization chamber, energy straggling in the entrance window and detector dead layers, and the finite spectrometer resolution. The corresponding corrections for energy losses in detector materials were estimated using stopping-power calculations, including SRIM [10]. For the present test measurements, the total uncertainty of the reconstructed mass peak positions is estimated to be of the order of 10%.

In addition, time-of-flight measurements of ^{252}Cf fission fragments were carried out to determine the fragment masses using the TOF technique. The obtained data clearly demonstrate the separation of fission fragments into two groups corresponding to light and heavy fragments. Figure 11 shows the two-dimensional spectrum of fission products in the energy versus time-of-flight coordinates.

The observed distribution has the typical structure expected for spontaneous fission fragments. Events corresponding to light fragments are located in the region of shorter time of flight, whereas heavier fragments are shifted toward larger TOF values. This behavior is consistent with the difference in fragment velocities after fission. The broadening of the groups is mainly caused by the intrinsic energy and mass distributions of ^{252}Cf fission fragments, energy losses in detector materials, angular spread, and the finite time and energy resolution of the spectrometer.

The separation of the light and heavy fragment groups confirms that the developed TOF $\Delta E - E$ spectrometer can be used for the registration of heavy fission products. These measurements also demonstrate the applicability of the selected detector configuration for further mass reconstruction of nuclear reaction products in experiments with heavy-ion beams. Thus, the ^{252}Cf test represents an important verification step before using the spectrometer in measurements of fission fragments and multinucleon transfer products produced in accelerator-based experiments.

Based on the measured values of the fragment time of flight and energy, the mass distributions of the fission fragments were reconstructed. As a result, the peak positions corresponding to the light and heavy fragment groups were determined to be $M_l = 116$ a.m.u. and $M_h = 140$ a.m.u., respectively. Figure 12 presents the mass distribution of ^{252}Cf fission fragments obtained in the present work in comparison with the results reported in Ref. [11], where the corresponding fragment masses were

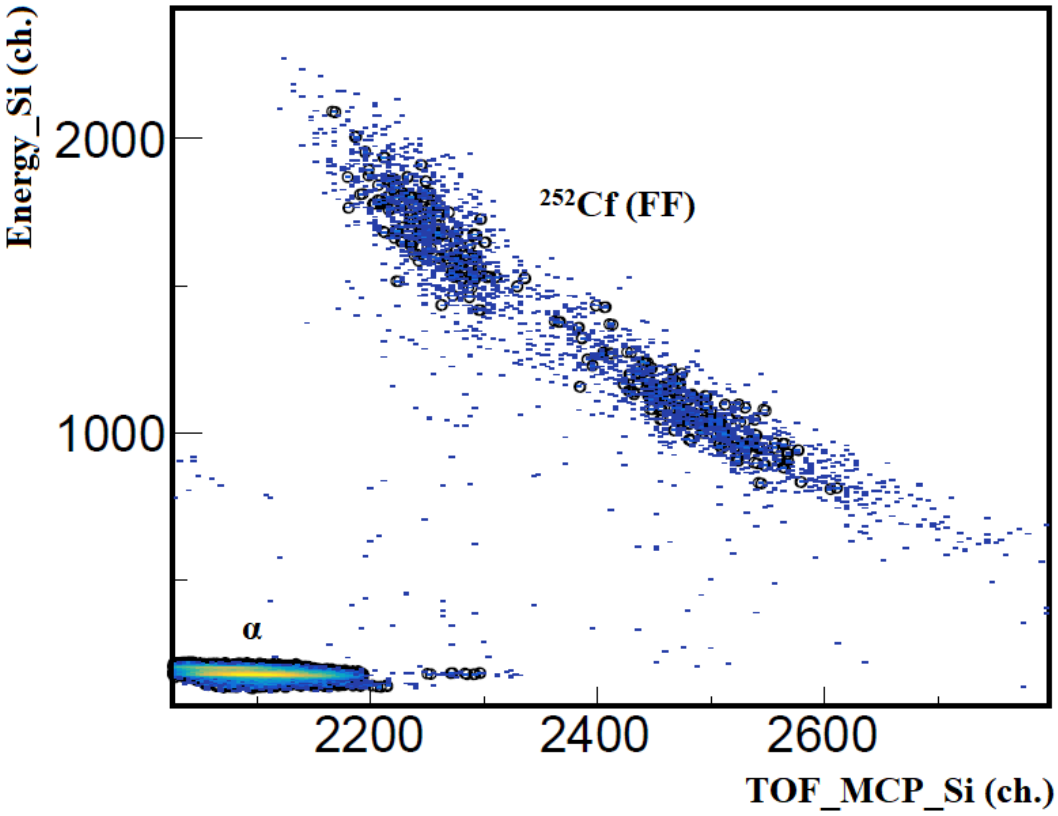

Figure 11: Two-dimensional spectrum of ^{252}Cf fission fragments in silicon-detector energy channel versus TOF channel coordinates.

found to be $M_l = 108.6$ a.m.u. and $M_h = 143.4$ a.m.u. The reconstructed mass distribution of ^{252}Cf fission fragments obtained in the present work is shown in Figure 12 together with the distribution reported in Ref. [11].

The peak positions obtained in the present work, $M_l = 116$ a.m.u. and $M_h = 140$ a.m.u., differ from the values reported in Ref. [11], where $M_l = 108.6$ a.m.u. and $M_h = 143.4$ a.m.u. were obtained. This difference may be attributed to differences in the experimental conditions and reconstruction procedures. In Ref. [11], the fragment masses and total kinetic energies were reconstructed event-by-event, corrections for prompt-neutron emission were applied, and the peak positions were determined by fitting the mass distribution with two Gaussian functions. In the present work, the fragment masses were reconstructed from the measured time-of-flight and energy values using the TOF–E method in a compact test spectrometer. Therefore, the reconstructed mass peak positions are sensitive to the time and energy calibrations, the flight-path length, energy losses in the MCP foil, entrance window, gas volume, and silicon-detector dead layers, as well as to the finite energy and time resolution of the system.

Taking into account the estimated mass uncertainty of about 10%, the observed displacement of the peak positions is within the expected accuracy of the present test configuration. Thus, the comparison with Ref. [11] should be considered mainly as a qualitative validation of the developed spectrometer. Nevertheless, the obtained distribution reproduces the characteristic double-humped structure of spontaneous fission of ^{252}Cf and demonstrates the possibility of separating the light and heavy

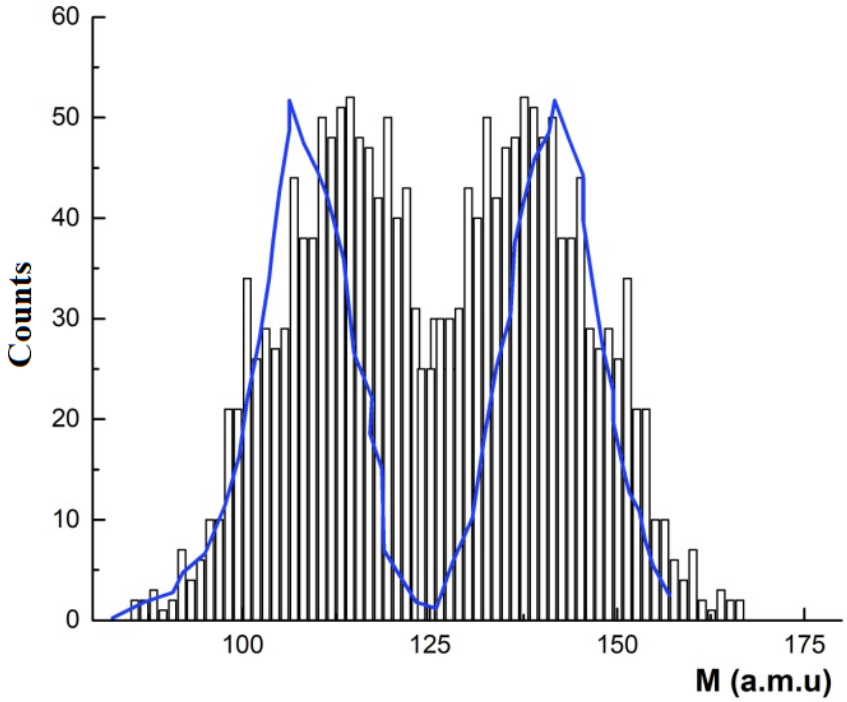

Figure 12: Mass distribution of ^{252}Cf fission fragments. The histogram represents the experimental data obtained in the present work. The blue line shows the distribution reported in Ref. [11].

fission-fragment groups.

Along with the ^{226}Ra source, a ^{252}Cf source was also used in the experiment and placed in front of the silicon detector. In the energy spectrum, four distinct α-lines from ^{226}Ra decay are clearly observed, as shown in Figure 13. At the same time, fission fragments from the ^{252}Cf source are registered and form a broad energy distribution. The known energies of the α-lines from ^{226}Ra were used for the energy calibration of the silicon detector, whereas the spectrum of ^{252}Cf fission fragments, measured in the absence of gas in the ionization chamber, provides a consistency check of the energy scale in the higher-energy region.

It is well known that the kinetic energies of ^{252}Cf fission fragments are typically on the order of 80–100 MeV. In the present measurements, the fragments pass through the entrance layers of the silicon detector, which leads to additional energy losses. As a result, the measured distribution is located in the range of approximately 55–85 MeV, which is in good agreement with the observed spectral position.

A two-dimensional distribution of fission fragments from the ^{252}Cf source in $\Delta E - E$ coordinates, obtained with the ionization chamber filled with pentane gas at a pressure of 7 Torr, is shown in Figure 14. The spectrum clearly exhibits a characteristic separation of heavy and light fission fragments, reflecting their difference in energy loss in the gas and residual energy measured by the ionization chamber and the silicon detector, respectively.

The observed separation is caused by the different masses, charges, and velocities of the fission fragments. Heavy fragments lose more energy in the gas volume due to their larger charge and lower velocity, whereas light fragments are characterized by different residual-energy values after passing through the ionization chamber. Thus, the $\Delta E - E$ spectrum provides an additional criterion for distinguishing between

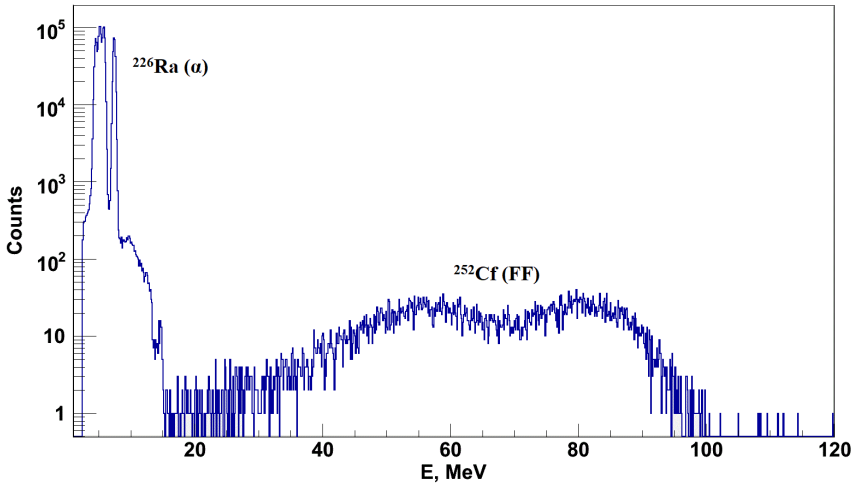

Figure 13: One-dimensional energy spectrum of α particles from the ^{226}Ra source and fission fragments (FF) from the ^{252}Cf source.

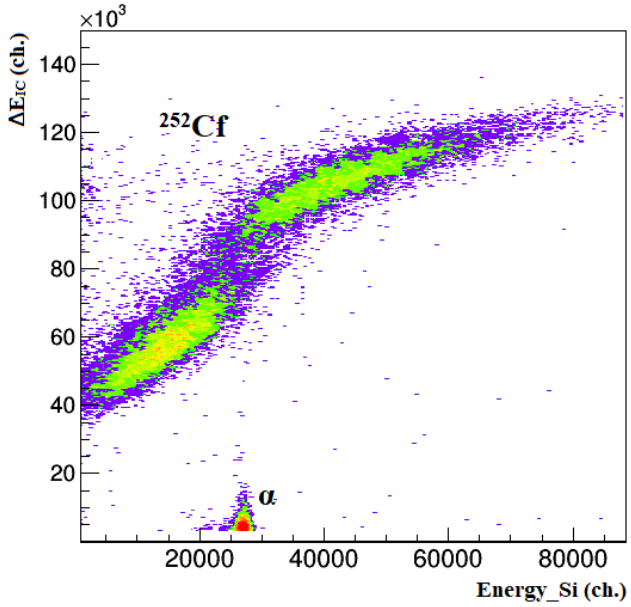

Figure 14: Two-dimensional distribution of fission fragments from the ^{252}Cf source in $\Delta E - E$ coordinates.

the two main groups of fission fragments.

These results confirm that the ionization chamber operates correctly as the energy-loss detector in the TOF $\Delta E - E$ spectrometer. The obtained two-dimensional distribution demonstrates the applicability of the developed detector system for simultaneous registration of fission-fragment energy loss and residual energy, which is necessary for further mass and charge identification of heavy nuclear reaction products.

4 Conclusion

In this work, a TOF $\Delta E - E$ spectrometer for charged particles was developed and tested. The system enables measurement of particle energy, time of flight, and

specific ionization losses, as well as determination of particle mass and charge.

Analysis of the obtained data confirmed the proper performance of the detector system. The calibration made it possible to determine the key parameters of the timing detectors and the ionization chamber and to evaluate the measurement accuracy. It was found that the resolution of the system is mainly determined by the characteristics of the microchannel-plate detectors, the accuracy of energy-loss measurements, and the operating conditions of the ionization chamber.

The estimated uncertainties, $\Delta Z/Z \approx 6$–8% and $\Delta M/M \approx 10\,\%$, for the present test configuration indicate that the developed spectrometer reliably separates groups of charged particles and fission fragments. At the same time, further improvement of the calibration procedure, optimization of the gas pressure, and more accurate correction for energy losses in detector materials are required for high-precision mass and charge measurements.

The measurements with ^{226}Ra and ^{252}Cf sources confirmed the possibility of registering light charged particles and separating light and heavy fission-fragment groups. The obtained spectra and two-dimensional distributions demonstrate the applicability of the developed setup to studies of heavy-nucleus fission processes. In future experiments, the spectrometer is planned to be used for the registration and analysis of fission fragments and multinucleon transfer products produced in heavy-ion reactions, including ^{40,48}Ca + ^{197}Au. This will expand the applicability of the method and provide new data on nuclear fission mechanisms and reaction-product formation.

Acknowledgments

The authors express their gratitude to I.V. Kolesov, B.A. Vorobyev, and I.V. Butusov for valuable discussions and assistance in the development and construction of several components of the spectrometer.

References

[1] E. M. Kozulin, A. A. Bogachev, M. G. Itkis *et al.*, Instrum. Exp. Tech. **51**, 44–58 (2008).

[2] K. D. Schilling, P. Gippner, W. Seidel *et al.*, Nucl. Instrum. Methods Phys. Res. A **257**, 197–208 (1987).

[3] P. Auger *et al.*, Z. Phys. A **289**, 255–259 (1979).

[4] D. Aznabaev, V. I. Smirnov, A. Isatov *et al.*, Phys. Part. Nucl. Lett. **16**, 620–626 (2019).

[5] I. V. Butusov, V. A. Maslov, K. Mendibayev, and A. V. Shakhov, JINR Preprint P3-2023-13, Dubna (2023) (In Russian).

[6] L. Heffern, *Ionization Chamber Design, Development, and Testing for the UNM Fission Fragment Spectrometer*, Master's thesis, University of New Mexico, Albuquerque, NM, USA (2015). Available at: `https://digitalrepository.unm.edu/ne_etds/46`

[7] LISE++ software package, available at: `https://lise.frib.msu.edu/lise.html`.

[8] R. Bimbot, H. Geissel, H. Paul, A. Schinner, and P. Sigmund, *Stopping of Ions Heavier than Helium*, ICRU Report 73, J. ICRU **5**, No. 1 (2005).

[9] R. Liguori Neto, N. Added, and F. A. S. Coutinho, Nucl. Instrum. Methods Phys. Res. B **161–163**, 159–163 (2000).

[10] J. F. Ziegler, M. D. Ziegler, and J. P. Biersack, *SRIM—The Stopping and Range of Ions in Matter*, Nucl. Instrum. Methods Phys. Res. B **268**, 1818–1823 (2010).

[11] D. David, J. Debrus, F. Lobke, H. Mommsen, R. Schoenmackers *et al.*, Phys. Lett. B **60**, 413–416 (1976).